Supplementary information

Enhanced the sensing performance of $WO_{2.72}$ to n-butanol via loading CeO_2 nanoparticles

Rong Wu[a&], Lu-Han Cheng[b], Chuan-Qi Ma[b], Zheng-Tao Yuan[b], Jiming Song[a,b]*

[a]School of Chemistry & Chemical Engineering, Anhui University, Key Laboratory of Structure and Functional Regulation of Hybrid Materials (Anhui University), Ministry of Education, Hefei, Anhui 230601, PR China.

[b]School of Materials Science and Engineering, Anhui University, Anhui Province Key Laboratory of Chemistry for Inorganic/Organic Hybrid Functionalized Materials, Hefei, Anhui 230601, PR China.

1 Experiment

1.1 Reagents

All chemicals are of analytical reagent quality. Tungsten chloride (WCl_6, 99.9%) is obtained from Macklin. Ltd. Glacial acetic acid ($C_2H_4O_2$, 99.5%), sodium hydroxide (NaOH, 96%), cerium nitrate hexahydrate ($Ce(NO_3)_2 \cdot 6H_2O$), 99.99%), formaldehyde (CH_2O, 99.5%), ethanol (C_2H_6O, 99.5%), ethylene glycol (EG, $C_2H_6O_2$, 99.5%), methanol (CH_4O, 99.5%), acetone (C_3H_6O, 99.5%), n-butanol ($C_4H_{10}O$, 99.5%), isopropanol (C_3H_8O, 99.7%) are available from Sinopharm Chemical Reagent Co., Ltd.

1.2 Fabrication and measurement of gas sensors

A certain amount of the above nanocomposite sample is taken into the agate, added with rosinols, and ground evenly until a paste is formed. The obtained paste is coated onto a pre-prepared ceramic tube (with two Au electrodes and four Pt wires). Finally, the ceramic tube inserted into the Ni-Cr heating coil is soldered to a hexagonal base to obtain the gas sensor. The as-prepared gas sensors are aged for 24 h in aging apparatus, after which the gas sensitivity is tested using WS-30A instrument. The corresponding liquid volume of VOCs is then taken with a micro syringe and injected into the heating table in the test chamber. The liquid on the heating table is evaporated into gas. A fan is turned on at the same time as heating to speed up the gas diffusion. The operating temperature for the duration of the test is controlled with the regulation of the voltage. The sensor response is defined as $S = R_a/R_g$, where R_a is the resistance in the atmosphere and R_g is the resistance in the mixture of the monitored

gas and air. Time of response and recovery are defined as the time when the sensor reaches 90 % of the total resistance change for the adsorption and desorption scenarios, respectively. During the test, the temperature is kept at 25℃ and the relative humidity (RT) is kept at 48%. The humidity of the test system is controlled through regulation of the content of the injected water droplets. Measurements of n-butanol sensing are performed as the relative humidity in the test chamber reaches the desired value.

1.3 Equipments and parameters

The X-ray diffraction analyses are conducted on a SmartLab diffractometer using CuKα radiation (λ=1.5418 Å) in the 2θ range of 20-60°. The Raman spectrometer (RM, inVia-Reflexa) and Fourier transform infrared spectroscopy (FT-IR, Vertex80+Hyperion2000) are employed to criticize the molecular structure and functional groups of the as-synthesized nanocomposites. The morphologies of the as-prepared samples are characterized with a scanning electron microscope (SEM, HITACHI, Regulus 8230). Moreover, a transmission electron microscope (TEM, JEM-F200), and a high-resolution transmission electron microscope (HRTEM) are used to examine the samples further, while energy dispersive X-ray spectroscopy (EDS) is employed to detect the presence of elements in the samples. S_{BET} and pore size distribution are resolved via Micromeritics ASAP 2460 surface analyzer. The elements and valence states present in the composites are detected via utilizing X-ray photoelectron spectroscopy (XPS, ESCALAB 250 electron spectrometer). The samples have been analysed by UV-visible diffuse reflectance spectroscopy using a

Lambda 1050 instrument. Then, an X-band benchtop electron paramagnetic resonance spectrometer (EPR, 2000 plus) is used to detect the g signal in the samples. The water contact angle was measured on a contact angle instrument (DSA30S) under ambient conditions.

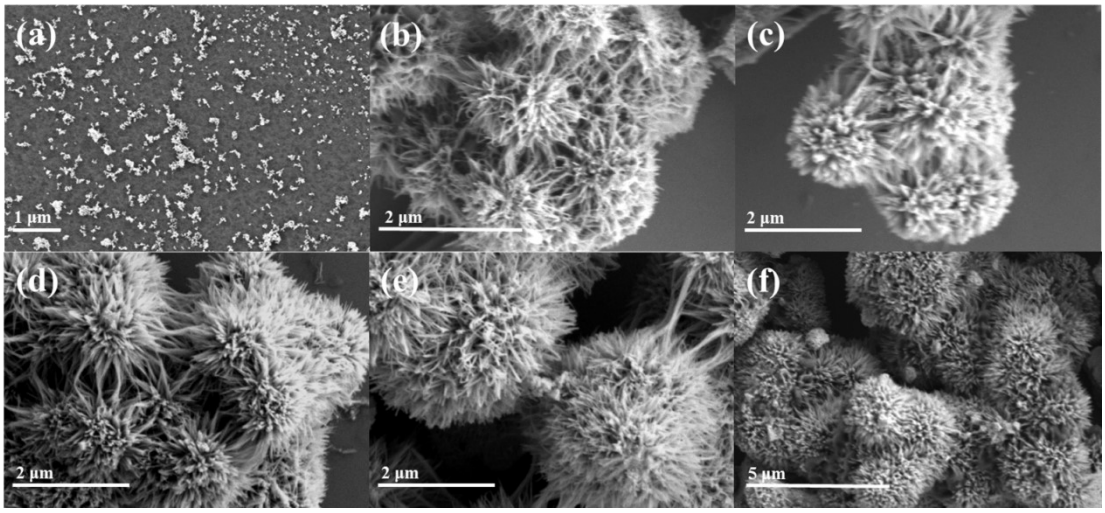

Fig. S1 SEM images of (a) CeO_2, (b) pristine $WO_{2.72}$, (c) $WO_{2.72}$-2.5 wt% CeO_2, (d) $WO_{2.72}$-5.0 wt% CeO_2, (e) $WO_{2.72}$-10 wt% CeO_2, (f) $WO_{2.72}$-20 wt% CeO_2.

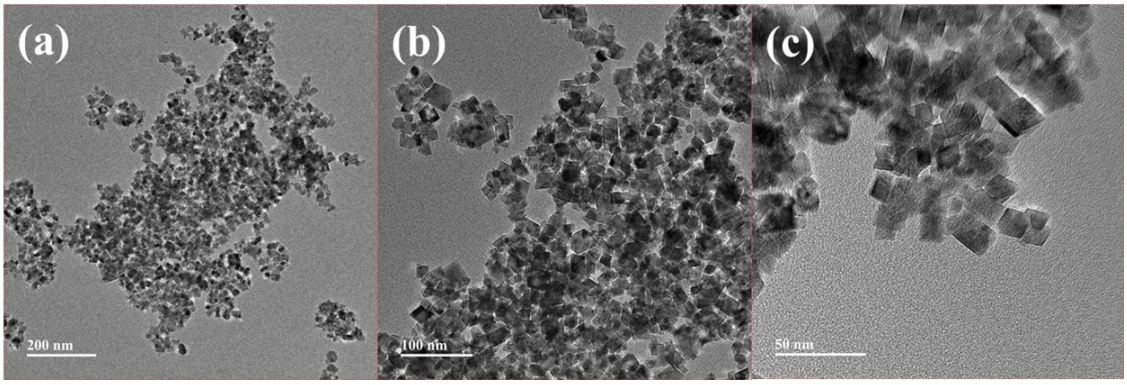

Fig. S2 TEM images of CeO_2 at different magnifications.

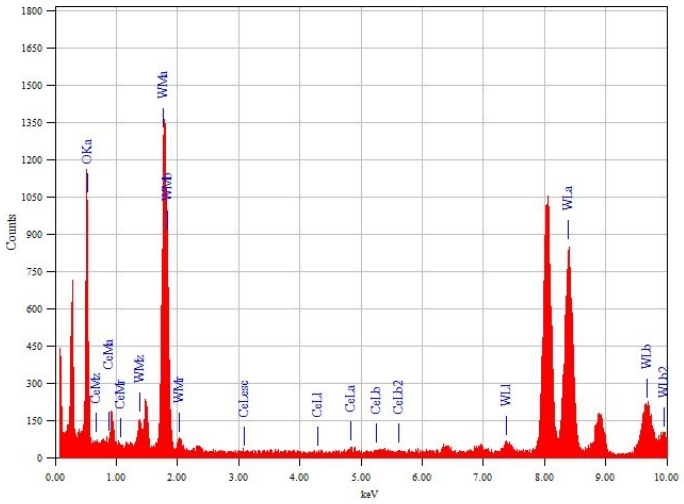

Fig. S3 The corresponding EDX spectrum from TEM of the $WO_{2.72}$-10 wt% CeO_2.

Fig. S4 XPS spectra of $WO_{2.72}$ (a) W 4f and (b) O 1s. O 1s spectra of (c) $WO_{2.72}$-2.5 wt% CeO_2, (d) $WO_{2.72}$-5.0 wt% CeO_2, and (e) $WO_{2.72}$-20 wt% CeO_2.

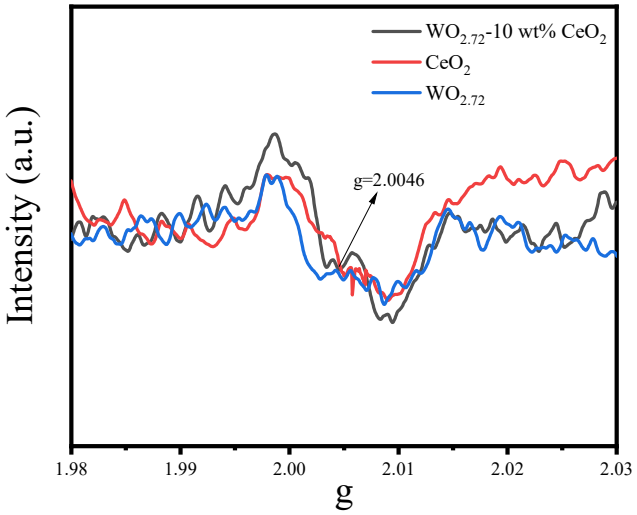

Fig. S5 The EPR spectra of CeO_2, $WO_{2.72}$ and $WO_{2.72}$-10 wt% CeO_2.

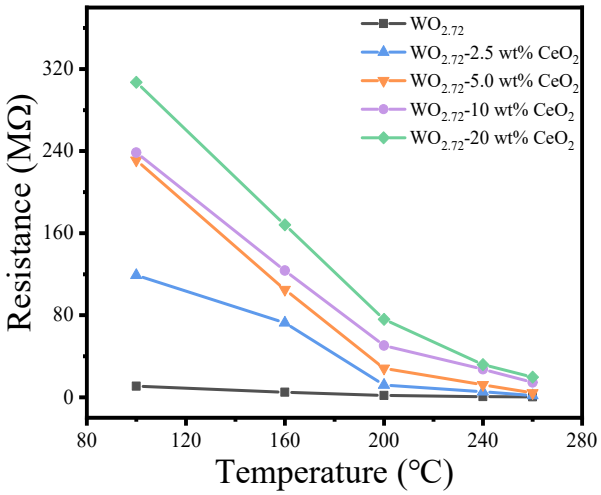

Fig. S6 The curves of the resistance of the $WO_{2.72}$-x wt% CeO_2 (x=0, 2.5, 5, 10, and 20) samples as a function of temperature.

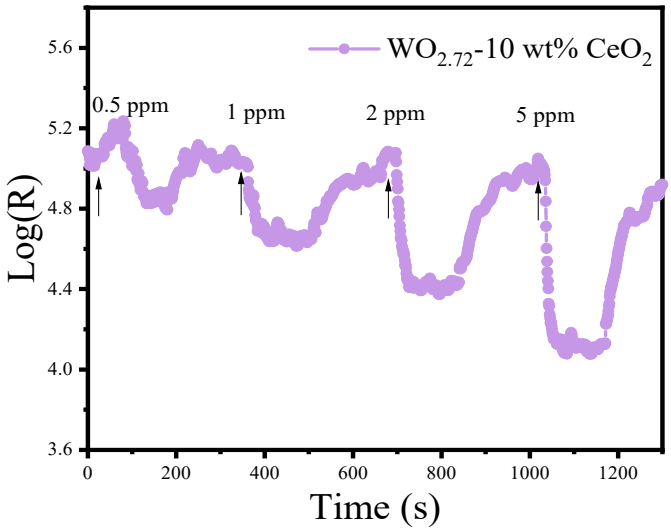

Fig. S7 The response of the $WO_{2.72}$-10 wt% CeO_2 sensor from 0.5 to 5 ppm n-butanol at 160℃.

Fig. S8 The response-recovery time transient curves $WO_{2.72}$-*x* wt% CeO_2 sensors for 5 ppm n-butanol at 160°C (a) *x*=0, (b) *x*=2.5, (c) *x*=5.0, (d) *x*=10 and (e) *x*=20. (f) Summary plot of response-recovery times for all samples.

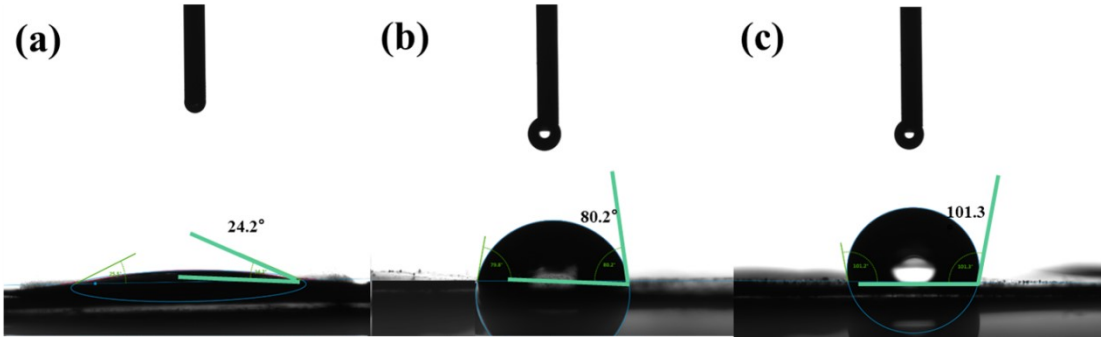

Fig. S9 WCAs of (a) $WO_{2.72}$, (b) $WO_{2.72}$-10 wt% CeO_2, and (c) CeO_2.